MECHANICAL BEHAVIOR AND DRY SLIDING WEAR RESPONSE OF AL-SI-SIC PARTICULATE COMPOSITE

[1]PAVAN KUMAR, [2]SANJAY SONI, [3]R. S. RANA, [4]ALOK SINGH

[1]Research Scholar, Department of Mechanical Engineering, MANIT, Bhopal, (M.P.), India
[2,3,4]Associate Professor, Department of Mechanical Engineering, MANIT, Bhopal, (M.P.), India
E-mail: sansoni_in@yahoo.com

Abstract- In the present investigation, an attempt has been made to study the mechanical behavior and sliding wear response of Al-Si alloy and Al-Si-SiC particulate composite developed by reinforcing 10 wt% and 15 wt% SiC particles of size 2µm in the Al matrix. Mechanical properties such as Tensile strength, Compressive strength, Impact strength, Hardness and Wear resistance of the composites were compared with the matrix alloy. The wear tests were conducted as a function of applied pressure and sliding distance. The response parameters such as wear rate, temperature rise, wear coefficient, seizure pressure, seizure temperature & COF were measured during the test. Microstructural examination of the alloy and the composite was carried out paying special emphasis to the distribution of SiC particle in Al matrix and interface bonding between SiC and Al matrix. Wear surface study was done in order to understand the mechanism of material removal during sliding wear. Fracture surface study was also done to see the mechanism of fracture occurring in the tensile test. Reinforcement of SiC particles into the matrix alloy was done by following Stir Casting technique. Specimens for specific tests were prepared as per international standards and fabricated by machining of the casted cylindrical fingers, ejected from the casting mould. Results show a large improvement in mechanical properties and wear resistance of the Al-Si-SiC particulate composite with 10wt% reinforcement. On further increase of reinforcement the properties tends to decrease due to high brittleness. The microstructural study of the alloy shows aluminum dendrites with dendretic arm spacing in the range of 25 microns. The eutectic silicon solidifies in the inter-dendretic region and around the dendrites. The microstructure of composite shows uniform distribution of SiC particles with good interface bonding. The tensile fracture study shows inter-granular fracture and SiC particle embedded on the surface. By careful observation of fracture surface it is depicted that particle decohesion and fracture both are occurring simultaneously in tensile fracture. Results concluded above can be useful for the industrial applications like aerospace, automobile and marine where mechanical and tribological properties of materials is an important concern.

Index Term- Al-Si Alloy; Al-Si-SiC particulate composite; reinforcement; wear; sliding distance; sliding speed; tensile strength; hardness; impact strength; tribology.

I. INTRODUCTION

A composite material is a 'material system' composed of a combination of two or more micro or macro constituents that differ in form, chemical composition and which are essentially insoluble in each other [1]. The motto to design metal matrix composites (MMCs) is to achieve high specific strength, high specific stiffness, and superior wear resistance. The attainable improvements in the properties are dependent on the intrinsic properties of composite constituents and the size, shape, orientation, weight fraction and distribution of the reinforcing phase in the metal matrix [2,5,6]. The ever-increasing demand of such materials in automobile and aerospace industries has lead to the development of aluminum matrix composite (AMCs) where Al is metal matrix [3,7,8].

Wear can be defined as "damage to a solid surface, generally involving progressive loss of material, due to relative motion between that surface and a contacting substance or substances"[10].

In many applications, metal matrix composites are subjected to sliding motion. Wear is associated with interactions between plastically deforming asperities (high spots) on the sliding surfaces, and leads to the simple equation:

$$Q = KW / H$$

Where, Q is the volume removed from the surface by wear per unit sliding distance, W is the normal load applied between the surfaces, and H is the indentation hardness of the softer surface. The constant K is termed the "Archard" wear coefficient, is dimensionless and always less than unity [09]. Many research works have been carried out to investigate the sliding wear properties of the AMCs reinforced with different types of reinforcements such as SiC, Al_2O_3, TiC, TiB_2 and graphite [2, 4]. In the present work, an effort has been made to study mechanical and wear properties with varying weight fraction of SiC particle reinforced AMCs developed with the help of two - step mixing method of stir casting technique.

II. EXPERIMENTAL WORK

2.1 Materials

Aluminium-Silicon alloy (ADC12) is selected as matrix alloys for synthesis of AMCs. The chemical compositions of aluminium alloy were analyzed using glow discharge spectrometer.

Table 1 Chemical Composition of ADC 12 alloy

Si	Mn	Zn	Mg	Cu	Fe	Ni	Al
10.93	0.13	0.95	0.12	2.17	0.73	0.18	Rest

Table 2 Properties of ADC12 alloy

Property	**ADC12 alloy**
Density, g/cm^3	2.76
Thermal Conductivity, W/mK	10-40 at 1100°C
Specific Heat, J/gK	96.2
Elastic Modulus, GPa	68.90
Coefficient of Thermal Expansion, K^{-1}	31.1x10^{-6}
Poison Ratio	0.33

2.2 Reinforcement

The SiC particles used as reinforcement in the aluminum matrix for synthesizing the composites are sieved using standard sieving practice through different grades of sieves in a vibratory sieving machine, with an aim to get particles within the size range of 2µm

Table 3 Properties of SiC reinforcement

Property	SiC Particles
Density, g/cm^3	3.2
Thermal Conductivity, W/mK	92
Specific Heat, J/gK	840
Elastic Modulus, GPa	420-450
Coefficient of Thermal Expansion, K^{-1}	4.3x10^{-6}
Poison Ratio	0.17

2.3. Composite Preparation

Melting of the ADC-12 alloy was carried out at temperature 780°C in graphite crucibles using a induction furnace. The composite was prepared by the stir casting method. The method comprises of dispersing the second phase particles on to the vortex of the molten alloy. The vortex was created with the help of a rotating mechanical stirrer. The speed of rotation was maintained around 500 to 600 rpm. The SiC particles of the size 2µm were heated to 600^{o}C in a graphite crucible in a muffle furnace. The SiC particles were introduced into the molten alloy by churning action of the stirrer. To obtain a uniform pattern of stirring a baffle is used in the melt along the sides of the crucible. It produces great amount of turbulence in the flow pattern and induces better mixing of the SiC particles in the aluminium alloy melt. After the complete addition of SiC particles, the speed of the stirrer is brought down to 200- 400 rpm and the stirring continued for 3-5 minutes. Now the temp of molten mixture is brought down to 680°C to provide ultrasonic vibration to mixture for proper mixing. When the alloy reaches semi pasty stage the surface is covered with a fluxing agent (coverall 11). About 7 g of flux is added to 1 kg of the molten alloy. The dross is removed from the surface of the melt using a refractory skimmer. The dissolved gases were removed by purging dry nitrogen gas into the melt for 5 minutes. After degassing, the surface is again cleaned and the temperature of the melt is increased to 760°C to take care of the minimum gas absorption during bubbling. The stirrer is then withdrawn from the melt. The composite melt was then solidified into a cast iron permanent die in the form of fingers.

2.4 Specimen Preparation

The specimens for various mechanical tests were prepared in accordance with the BIS/ASTM codes mentioned in the table 4.

Table 4

Test	Code	Dimension	No. of specimens
Tensile	IS 1608	10mmØ	3
Compressive	IS 1757	L/D 1.5 -2.0	3
Impact	IS 1501	55x10x10 V Notch 2mm depth	3
Hardness	IS 1586	15mmØ,L=15 mm	3
Wear	ASTM G40	8mmØ ,L=30mm	6

2.5 Mechanical Testing

The specimens were tested at room temperature for various tests. Mechanical properties such as UTS and Compressive strength were evaluated on computerized Universal testing machine (INSTRON M/c, Model 5586) 400KN Capacity at a strain rate of 0.5 mm/min. Hardness and Impact strength were evaluated on Analog Rockwell hardness tester (FIE make, model VM 50) and Charpy Impact Tester (FIE make, model FIT 30) at MANIT, Bhopal.

2.6 Wear Testing

The sliding wear tests were performed using Pin on Disc tester (DUCOM make, model TR-20LE) at different load conditions for 5000m run. Sliding wear behavior was studied as a function of applied pressure and sliding distance at a speed of 4.4 m/sec. The response parameters such as wear rate, wear coefficient, seizure pressure, seizure temperature & coefficient of friction were measured during the test. The tests were conducted till the Seizure of the specimen was observed. The wear rates (m^3/m) of the

samples were calculated on the basis of Volume loss. Finally the worn specimens were examined using SEM (JEOL make, Model JSM-6390) for wear surface study.

2.7 Microstructural Examination

Samples for microstructural characterization were polished according to standard metallographic procedures. Various steps involved during the process were polishing the specimens with different grade of emery papers and then finally with fine polishing alumina using polishing cloths. The samples were etched with Keller's reagent and observed in a SEM.

2.8 Fracture Surface Study

For fracture surface study the fractured tensile specimens were cut, cleaned with acetone and fixed on a copper holder using double sided copper tape and coated with platinum, before keeping under observation through a scanning electron microscope.

III. RESULTS AND DISCUSSION

3.1 Mechanical Properties

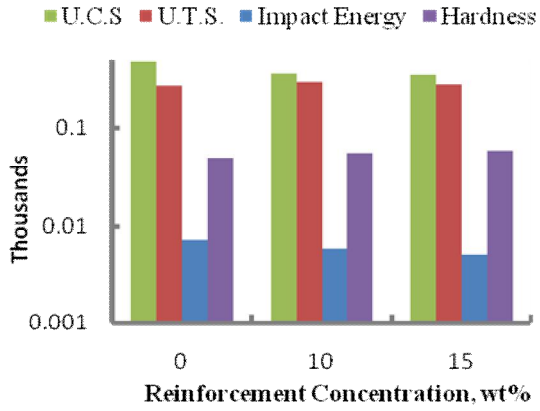


Fig 3.1 showing comparision of various mechanical properties of alloy and the composites

Fig (3.1) shows the variation of tensile strength of the alloy and the composites with different weight percentage of reinforcement. It is noted from the figure that the tensile strength value was 281.13 MPa for alloy which increases to 299.97 MPa for 10% SiC composite. On further increases in SiC reinforcement the tensile value decreases to 283.04 MPa. So it is observed here that there is an improvement of around 7% in the tensile strength in case of 10% SiC composite and almost same in 15% SiC composite. It is understood that dispersion of fine SiC particles of size (2µm) in aluminium alloy matrix tends to reduce the tensile properties as during tensile deformation the soft aluminium matrix will elongate and the SiC particles which are very hard are not deformed at the same rate as the matrix does. This non uniform deformation of matrix and hard particles results into development of cracks at the interface. Hence decohesion and void formations are the main reason for lowering the tensile strength of aluminium alloy particle composites then the aluminium alloy. This fact is also verified from the fracture surface study of the materials.

Also fig (3.1) shows the variation of Compressive strength of the alloy and the composites. It is noted from the figure that Compressive strength value was 484.39 MPa for alloy which decreases to 373.39 MPa for 10% SiC composite and on further increases in SiC reinforcement to 15%, the Compressive strength value decreases to 353.04 MPa. So it is observed here that there is decrease in compressive strength with increase in SiC percentage.

It is understood that dispersion of SiC particles in aluminium alloy matrix tends to reduce the compressive properties as during compression the soft aluminium matrix will compress and the SiC particles which are very hard are not deformed at the same rate as the matrix does. This non uniform deformation of matrix and hard particles results into development of cracks at the interface, hence lowering the compressive strength of aluminium alloy particle composites.

Fig (3.1) also shows the variation of hardness of the alloy and the composites. It is noted from the figure that hardness of the composite increases with increase in concentration of SiC particles. The value of hardness being 50 HRB for alloy which increases to 55 HRB for 10% SiC composite and 58 HRB for 15% SiC composite.

There is an improvement of around 10% and 16% in the hardness of the composites as compared to the alloy. The dispersion of SiC particles in aluminium alloy offer resistance to deformation of the matrix. A good interface between the SiC and aluminium matrix always give rise to higher hardness value. Incorporation of 15% SiC particles in aluminium matrix shows highest hardness values amongst all.

Fig (3.1) also shows the variation of impact strength of the alloy and the composites. It is observed from the figure that the impact strength for alloy was 7.3 Nm which decreases to 5.7 Nm and 5.0 Nm respectively for 10% and 15% SiC composite. The impact strength value indicates that impact strength decreases with increase of SiC concentration in the composites. It is quite understandable that dispersing hard ceramic particles in soft matrix reduces the energy absorption capability of the material. More is the dispersion of SiC particles lesser is the impact strength. When there is sudden impact, the interface between the particles and the matrix breaks and decohesion produces new surfaces and the energy is released. On the other hand in the case of aluminium alloy the matrix material absorb the impact energy without fracturing.

3.2 Wear Testing

Sliding wear behavior of Al-alloy and composite was studied as a function of applied pressure and sliding distance. The response parameters such as wear rate, temperature rise, wear coefficient, seizure pressure, seizure temperature & COF were measured during the test.

3.2.1 Effect of Applied Pressure on Wear Rate

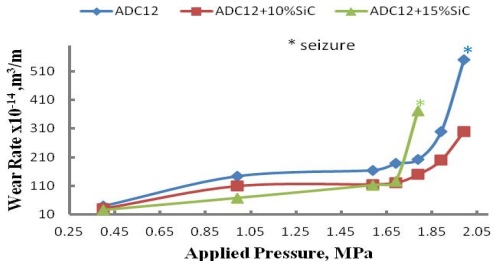


Fig 3.2 Effect of Applied Pressure on Wear Rate at Sliding Distance of 1000 m

Fig (3.2) shows the wear rate of ADC12 alloy and the composite as a function of applied pressure at a sliding velocity of 4.4 m/sec. It is observed from the figures that the wear rate initially increases slowly with increase in applied pressure irrespective of the material and at a later stage beyond certain applied pressure, the wear rate shoots up very rapidly. For example the wear rate of alloy at an applied pressure of 0.40 MPa is $4X10^{-13}$ m^3/m which increases to $1.44X10^{-12}$ m^3/m at an applied pressure of 0.99 MPa. On further increase in applied pressure the wear rate increases to $2.03x1^{-12}$ at an applied pressure of 1.79 MPa. On further increase in applied pressure the alloy seizes at 1.99 MPa. Similar trends were observed for composites, for 10%SiC composite at an applied pressure of 0.40 MPa the wear rate was $3x10^{-13}$ m^3/m which increases to $1.09x10^{-12}$ m^3/m at an applied pressure of 0.99 MPa. On further increase in applied pressure the wear rate increases to $1.5 x10^{-12}$ m^3/m at an applied pressure of 1.79 MPa. On further increase in applied pressure the composite seizes at 1.99 MPa. For 15% SiC composite, the wear rate at an applied pressure of 0.40 MPa was $2.6X10^{-13}$ m^3/m which increases to $6.8X10^{-13}$ m^3/m at 0.99 MPa. On further increase in applied pressure the wear rate increases to $1.25x10^{-12}$ m^3/m at an applied pressure of 1.69 MPa. On further increase in applied pressure the composite seizes at 1.79 MPa. So it is very clear from the values that the wear rate for a certain range is constant but shoots up rapidly before theses gets seized. The pressure at which wear rate increases suddenly to a very high value is termed as transition pressure and the pressure at which material gets seized is known as seizure pressure. Here the transition pressure and seizure pressure for all the materials is noted to be almost same. It is further noted that the wear rate is least in case of 15% SiC composite $2.6X10^{-13}$ m^3/m at 0.40 MPa and maximum for alloy which is $5.5X10^{-12}$ m^3/m at 1.99 MPa.

3.2.2 Effect of Applied Pressure on the Temperature at End of Test Run

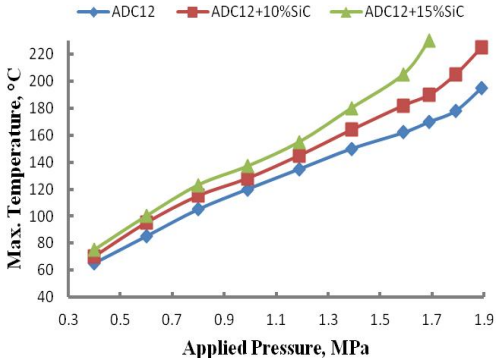


Fig 3.3 Maximum Temperature obtained for the specimens during wear test at various Applied Pressure and 5000m sliding distance

Fig (3.3) shows the variation of maximum temperature, obtained at the end of test run of 5000m, as a function of applied pressure for various materials. It is evident from the figure that the maximum temperature increases with increase in applied pressure. As pressure increases, the fractured SiC particles between the contact surface of specimen and disc increases which results in increase of frictional heating and temperature. Frictional heating increases with the concentration of reiforcement at identical wear test condition. The above values indicates that composites are more thermally stable.

3.2.3. Effect of Applied Pressure on Coefficient of Friction

The variation of coefficient of friction for alloy is shown in fig (3.4) It is noted from the figure that the coefficient of friction for the alloy varies up & down within a narrow band with increase in applied pressure. The range of coefficient of friction is primarily between 0.07 to 0.13.

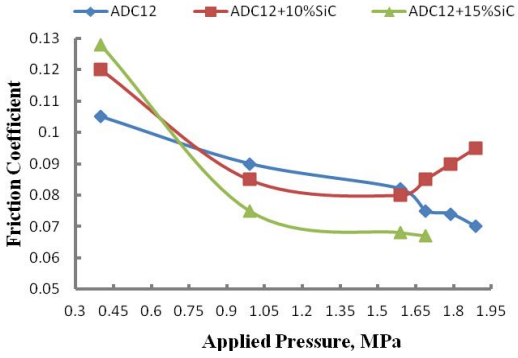


Fig 3.4 Showing Coefficient of Friction during sliding wear at varying applied pressures and 3000m sliding distance

3.2.4 Effect of Applied Pressure on Wear Coefficient

Wear coefficient is basically probability of forming wear debris. The wear coefficient for alloy and composites at a sliding speed of 4.4 m/sec at different

applied pressure is shown in fig (3.5). It is noted from the figure that the wear coefficient was initially more but decreases with applied pressure up to a certain value of applied pressure but increases suddenly when the applied pressure reaches near to seizure of the specimen. This is understood as work hardening of the alloy is taking place initially but at high applied pressure the wear increases because at high load regime there is a every possibility of formation of sub surface cracks which join together and lead to higher wear by formation of plate shaped debris. It is further noted that the wear coefficient for the alloy lies in the range of 10^{-3}.

Even at the seizure pressure the value of wear coefficient is in the range of 10^{-3} which signifies that the type of wear in ADC12 alloy corresponds to severe wear. The wear coefficient for 10% SiC and 15% SiC composites remains almost constant in a narrow range and increases suddenly when the applied pressure reaches near to seizure of the specimen. The value of wear coefficient for composites is in the range of 10^{-4} which corresponds to mild or oxidational wear condition. Above fact indicates that dispersion of SiC particles in ADC 12 alloys reduces the wear coefficient values.

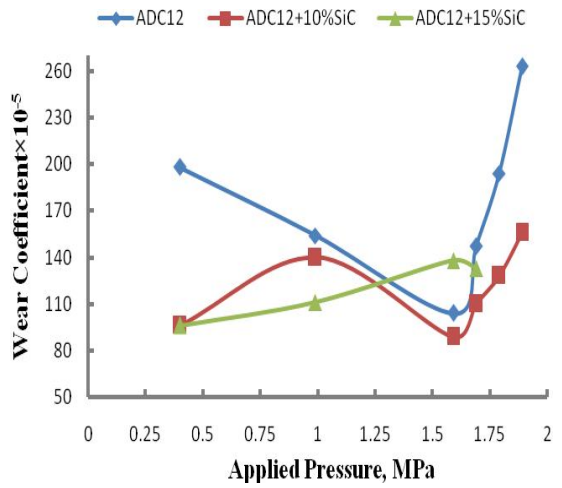


Fig 3.5 Showing Wear Coefficient with Applied Pressure in alloy and the composites.

3.3 Microstructural Study

3.3.1 Microstructure of ADC12 Alloy

Microstructure of Aluminum silicon alloy (ADC12 alloy) solidified in a cast iron mold shows aluminum dendrites with dendretic arm spacing in the range of 25 microns.

The eutectic silicon solidifies in the inter-dendretic region and around the dendrites (fig 3.6). The higher magnification micrograph (fig 3.7) depicts plate shaped eutectic silicon and the other intermetallic phases. The plate shaped eutectic silicon is usually 20-30 micron in length and 2-5 micron in width. In some instances the eutectic silicon are needle shaped.

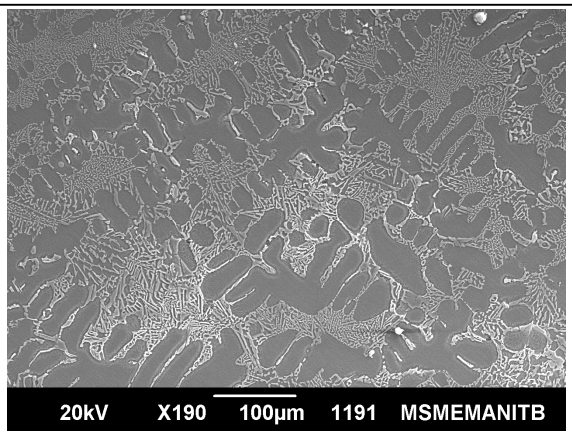


Fig 3.6 SEM micrograph showing silicon solidifying in the inter-dendretic region and around the dendrites.

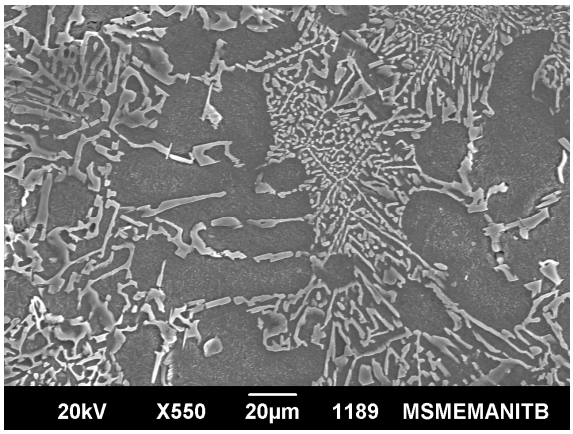


Fig 3.7 SEM micrograph showing plate shaped eutectic silicon and the other intermetallic phases.

3.3.2 Microstructure of SiC Composite

Fig 3.8 shows the micro structure of SiC composite, it shows the secondary aluminum dendrites with eutectic silicon in the dendretic spacing and around the dendrites and SiC particles are seen distributed in the matrix. It is to be noted that the SiC particle feature in the range of 2 micron are usually pushed by the aluminum dendrites into the last freezing eutectic liquid. A higher magnification micrograph shows the entrapment of SiC particles in the last freezing eutectic liquid with good interface bonding.

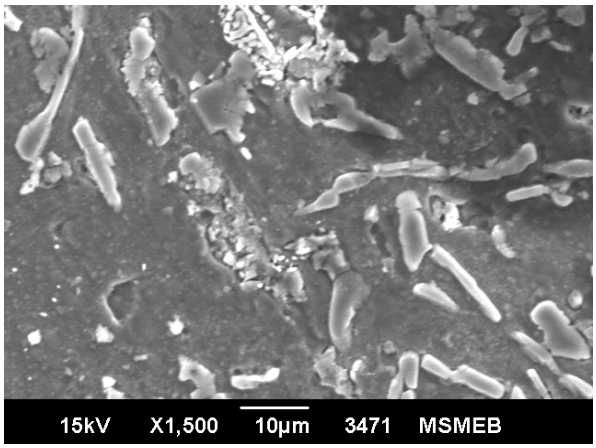


Fig 3.8 SEM micrograph showing distribution SiC particles in the composite.

3.4 Wear Surface Study

The wear surface of alloy and the composites was studied using Scanning Electron Microscope (SEM). In order to understand the mechanism of material removal during sliding wear, the worn surfaces of wear specimens were cut, cleaned with acetone and fixed on a copper holder using double - sided copper tape and coated with platinum, before keeping under observation through a Scanning Electron Microscope.

3.4.1 Wear Surface Study of ADC 12 Alloy

The wear surface of ADC 12 alloy at a sliding speed of 4.4 m/sec was studied under SEM. It showed that during the sliding wear, there is asperity to asperity contact between the sliding surfaces. The harder asperity, the steel surface in this case (62 HRc), slides over the softer aluminum surface and results into formation of grooves. A typical wear surface of ADC 12 Alloy at a pressure of 0.40 MPa is shown in fig (3.9). This figure also shows some damaged regions. It is interesting to note that during the sliding action, cracks are formed on the surface which propagates along the longitudinal as well as transverse directions fig (3.10),(3.11). It is noted that transverse cracks join the grooves together. At this pressure, the wear surface is damaged in such a manner that it forms finer sized debris particles. On increasing the pressure to 0.99 MPa, the depth of grooves is increased and more damaged regions are observed fig (3.12). Further increasing the pressure to 1.99 MPa, the sample tends to seize and the wear surface is characterized by the formation of parallel lips fig (3.13). At higher pressure, the material softens because of temperature, and tends to weld on a micro-scale.

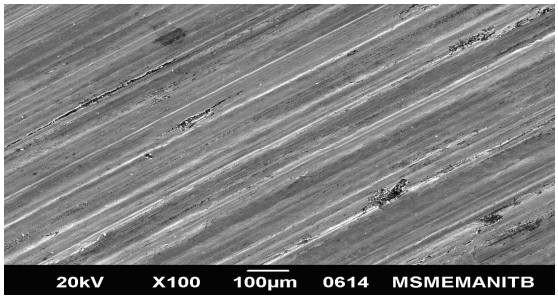


Fig 3.9 SEM micrograph showing a typical wear surface of ADC 12 alloy at a pressure of 0.40 MPa.

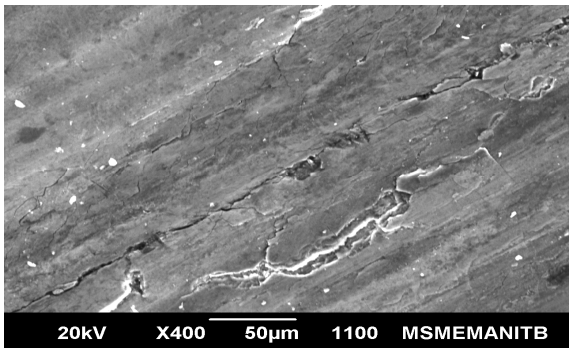


Fig 3.10 SEM micrograph showing cracks formation on the surface which propagates along the longitudinal directions.

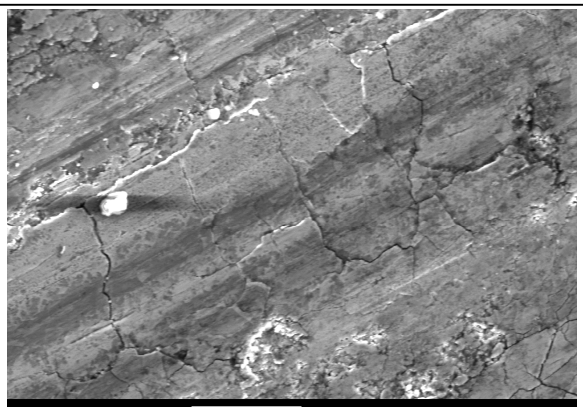


Fig 3.11 SEM micrograph showing cracks formation on the surface which propagates along the transverse directions.

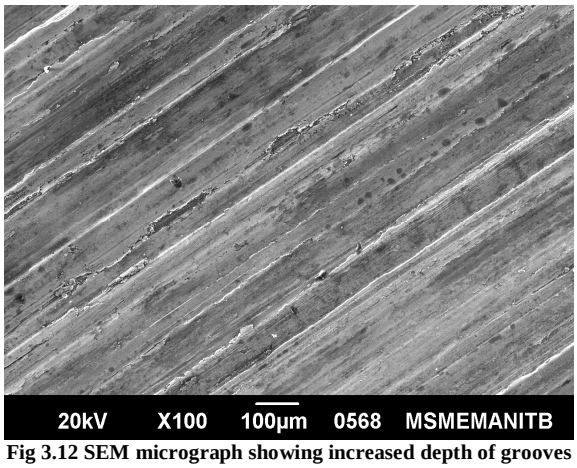


Fig 3.12 SEM micrograph showing increased depth of grooves at 0.99 MPa applied pressure.

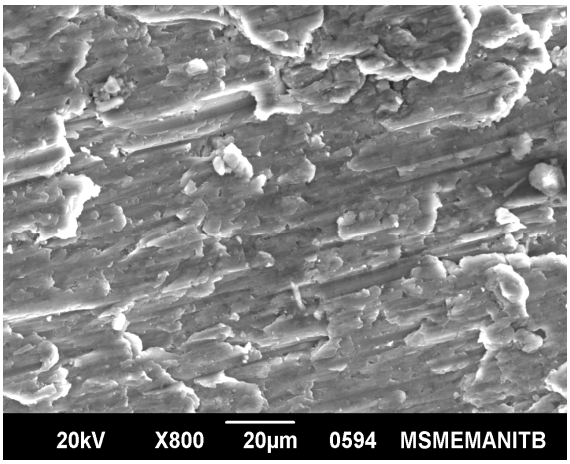


Fig 3.13 SEM micrograph showing seizure of the specimen and the wear surface is characterized by the formation of parallel lips.

3.4.2 Wear Surface Study of Composite

The wear surface of SiC composite shows similar features as those of alloy. (Fig.3.14) shows a typical wear surface of ADC12 10% SiC composite at pressure of 0.40MPa. It also shows continuous grooves and pittings. It is to be noted that the appearance of pitting in ADC12-SiC composites is a common feature observed. This may be due to the presence of hard particles and soft matrix inter-

phases. On increasing the pressure to 0.99 MPa, the wear surface is characterized by deep wear grooves and pitting (Fig.3.15). A higher magnification micrograph (Fig.3.16) shows pitting and longitudinal & transverse cracks on the wear surface. At higher pressure, initiation and propagation of cracks is prominent. When these cracks are joined together, they form a flaky shaped debris . Further increasing the pressure to 1.99 MPa, the sample gets seized which is in general characterized by formation of parallel lips (Fig.3.17).

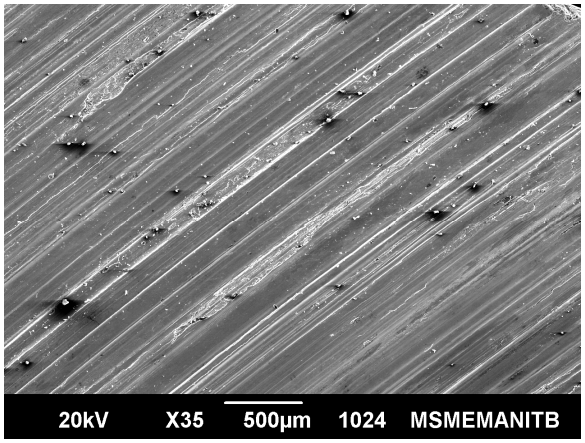


Fig 3.14 SEM micrograph showing typical wear surface of ADC12 10% SiC composite at pressure of 0.40 MPa. It also shows continuous grooves and pittings.

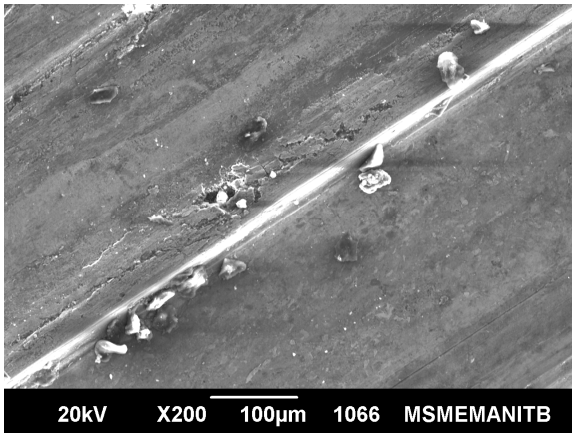


Fig 3.15 SEM micrograph showing deeper grooves and pitting at 0.99 MPa applied pressure.

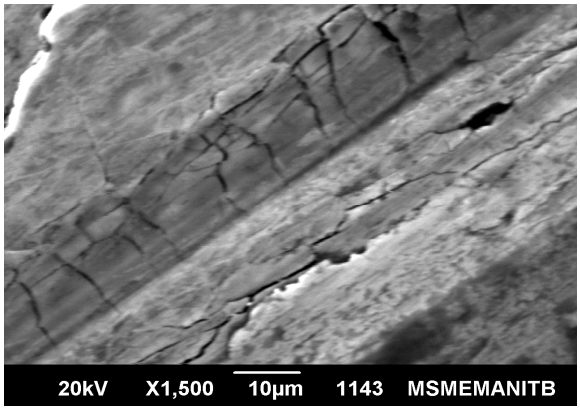


Fig 3.16 SEM micrograph at higher magnification showing longitudinal & transverse cracks on the wear surface.

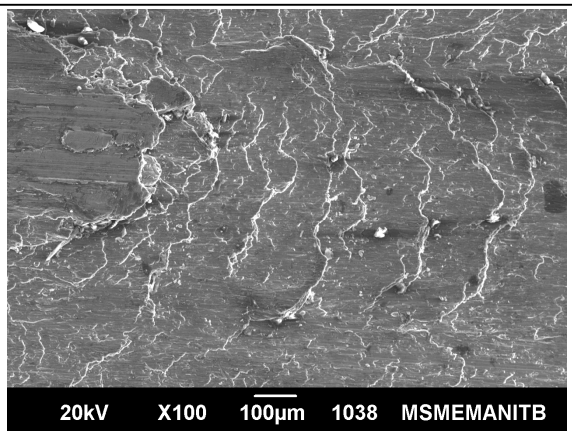


Fig 3.17 SEM micrographs showing seizure of composite characterized by formation of parallel lips.

3.5 Mechanism of Material Removal

The typical SEM photograph of a wear surface shows the continuous grooves running from one end of the sample to the other end. This happens when the hard asperities of the counter surface (in the present case it is steel surface) scratches the softer surface (in this case it is aluminium) and produces continuous grooves. The depth of grooves depends upon the applied pressure used during the wear test. The width of the grooves is dictated by the width of the asperities of harder surface. In the initial stage there is a asperity to asperity contact and during the sliding action the softer asperity is broken down by the interaction with the harder asperity and later on there will be a direct contact between the harder asperities and softer surface. During the sliding action there will be a groove formation on softer surface which results into work hardening of the Al surface. In the initial stage the wear of material is dictated by the scratching action. On prolonged sliding action the asperities of the hard surface will also be broken down and a situation comes when there will be a direct surface to surface contact. This leads to formation of oxide layer more on the softer Aluminium surface and the black colour oxide surface is discernable.

This happens in the mild wear regime. Further the oxide layer will be removed by continuous sliding action. Further enhancing the applied pressure the stress on the softer surface will be more which leads to breaking of oxide layer and fresh surface will be evolved. At high load regime there is a every possibility of formation of sub surface cracks which join together and lead to higher wear by formation of plate shaped debris. The wear surface at high load regime is more of damaged regions. Further enhancing the load the friction become higher and the temperature also increases to a higher level which leads to incipient melting at the contact junctions. This melting results into sticking behavior of the materials and not allowed for free sliding action. This phenomenon is called the inception of seizure. The wear surface at the time of seizure is represented by

parallel lips formation. In case of composites the hard SiC particles offers resistance to the wear and thus the wear is less in case of composites.

3.6 Fracture Surface Study

The fracture surface study was done to ascertain the type of fracture taking place in the alloy and the composite. In case of aluminum silicon alloys, aluminum is a ductile material which fracture in ductile manner having considerable amount of plastic deformation on the other side silicon is a metalloid which fracture by brittle manner. In Al-Si alloy, silicon is preferentially segregated around the aluminum dendrites and provide easy path for crack nucleation and propagation. In Al-Si alloy the fracture is taking place by inter- granular manner (crack propagation along the grain boundary). When we observe the fractograph of Al-Si alloy it shows the morphology of dendrites in the fracture surface.

ADC 12 -10% SiC composite shows similar features indicating inter-granular fracture and SiC particle embedded on the surface. In the case of composite the fracture may take place by decohesion of particle matrix interphase or it may be due to particle fracture. By careful observation of fracture surface it is depicted that particle decohesion and fracture both are occurring simultaneously in tensile fracture (fig 3.19). In some instances the segregation of particle in aluminum matrix is also observed.

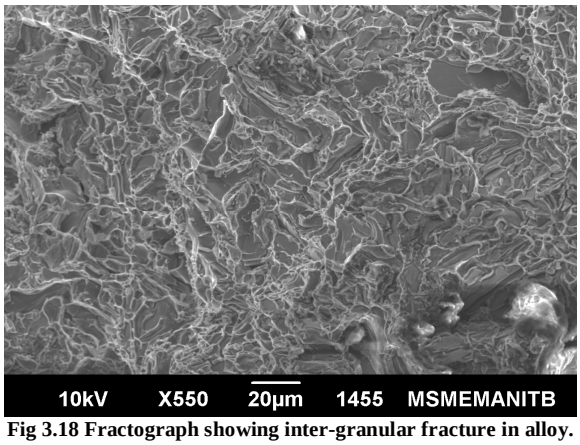


Fig 3.18 Fractograph showing inter-granular fracture in alloy.

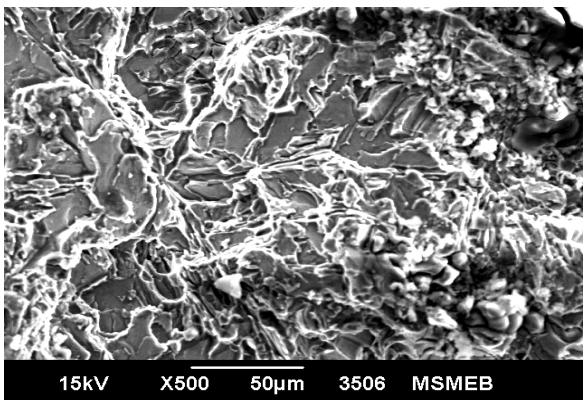


Fig 3.19 Fractograph showing particle decohesion and inter-granular fracture in composite.

CONCLUSIONS

The experimental study reveals following conclusions:

1. Tensile strength of composite increases for 10% SiC composite but remains equal to alloy in 15% SiC composite.

2. Compressive strength of composites decreases with increase in SiC concentration.

3. Hardness of the composites increases with increase in SiC concentration.

4. Impact strength of composites decreases with increase in SiC concentration.

5. The wear rate increases with increase in sliding distance and applied pressure for all the materials.

6. The coefficient of friction varies in the range of 0.07 to 0.13 for alloy and the composites.

7. The seizure pressure is more for composites as compared to base alloy.

8. The seizure temperature increases with increase in SiC concentration.

9. The wear coefficient of alloy lies in the range of 10^{-3} which signifies that type of wear is severe wear whereas in case of composites it is in the range of 10^{-4} which signifies that type of wear is mild or oxidational.

10. The microstructure of alloy shows aluminium dendrites and plate shaped eutectic silicon. Microstructure of composites shows uniform distribution of SiC particles in the base alloy with good interface bonding between the matrix alloy and the SiC particle.

11. Sliding wear mechanism: The stages associated with sliding wear are

(1) contact of the counter surfaces primarily at the asperities (ii) asperity-asperity interaction, deformation and fracture of asperities, micro grooving by higher and stronger asperities leading to formation of fewer wear debris which get entrapped in the wear track, and surface of the pin and counter surface (iii) oxidation of wear debris and surfaces of pin and counter surface, (iv) compaction and mixing of wear derrises with the surface material of pin and counter surface. (v) thermal and plastic incompatibility in addition to frictional heating and frictional force(shear force) leads to longitudinal and transverse cracking of material.

12. Fractograph shows that for alloy fracture is taking place by inter- granular manner and in case of composites it is by both, particle decohesion and fracture, simultaneously.

ACKNOWLEDGEMENTS

The authors would like to thank Director, MANIT, Bhopal for the facilities extended to carry out the present research work.

REFERENCES

[1] Manoj Singla, Lakhwir Singh, Vikas Chawla, Study of Wear Properties of Al-SiC Composites, Journals of Minerals and Materials Characterization and Engineering, 2009, vol.8, No.10, pp.813-819.

[2] Umakanth K, Selvamini S.T., Palanikumar K, Friction and Wear Behavior of Al6061 Alloy (SiC_p+Al_2O_{3p}) Hybrid Composites, International Journal of Engineering Science and Technology, 2011, vol. 3, no.7.

[3] N. Natarajan, S. Vijayarangan, I. Rajendran, Wear behaviour of A356/25SiCp aluminium matrix composites sliding against automobile friction material, Wear, 2006, pp.812-822.

[4] Yang,J.B., Lin,C.B., Wang,T.C., and Chu.H.J., "The Tribological Characteristics of A356.2Al alloy/Gr_p_ Composites," Wear, 2004, 257, pp 941– 952.

[5] Rajaneesh N. Marigoudar, Kanakuppi Sadashivappa, Dry Sliding Wear Behaviour of SiC Particles Reinforced Zinc-Aluminium (ZA43) Alloy Metal Matrix Composites, Journal of Minerals & Materials Characterization & Engineering, 2011, Vol. 10, No.5, pp.419-425.

[6] K. Ravi Kumar, K. M. Mohanasundaram, G. Arumaikkannu, R. Subramanian, Influence of Particle Size on Dry Sliding Friction and Wear Behavior of Fly Ash Particle–Reinforced A 380 Al Matrix Composites, European Journal of Scientific Research, 2011, Vol.60 No.3, pp.410-420.

[7] G. B. Veeresh Kumar, C. S. P. Rao, N. Selvaraj, Mechanical and Tribological Behavior of Particulate Reinforced Aluminum Metal Matrix Composites – A review, Journal of Minerals & Materials Characterization & Engineering, 2011, Vol. 10, No.1, pp.59-91.

[8] S. Venkat Prasat, R. Subramanian, N. Radhika, B. Anandavel, Influence of parameters on the Dry Sliding Wear Behaviour of Aluminium/Fly ash/Graphite Hybrid Metal Matrix Composites, European Journal of Scientific Research, 2011, Vol.53 No.2, pp.280-290.

[09] J.F. Archard, J. Appl. Phys., 24 (1953) 981-988.

[10] E. Rabinowicz, Friction and Wear of Materials, John Wiley and Sons Inc(1965).

★★★